Interaction between NO and C_2H_4 on Rh-Loaded $CeO_X(111)$

D. R. Mullins* and K. Zhang

Oak Ridge National Laboratory, Oak Ridge, Tennessee 37831-6201

Received: October 18, 2000; In Final Form: December 11, 2000

The interaction between NO and C_2H_4 was studied on ceria-supported Rh model catalysts (Rh/CeO_X). When the ceria is fully oxidized the primary reaction products observed in TPD are NO, N_2, CO, and H_2O. This is similar to what is observed on Rh(111) except that CO results from the reduction of the CeO_2 by the C in the C_2H_4. On highly reduced ceria the only hydrogen-containing products are H_2 and a small amount of NH_3. The O that comes from NO decomposition on Rh migrates to the CeO_X before H_2O formation occurs. N_2 and CO desorb from Rh/CeO_X at a higher temperature than from Rh/CeO_2. Soft X-ray photoemission indicates that the NO and C_2H_4 do not strongly interact to form new intermediates on Rh/CeO_2. As the molecules decompose they produce N and C atoms on the surface, which eventually react to form N_2 or CO. The C and N do combine on reduced Rh/CeO_X. CN is formed between 400 and 500 K. The CN produces more complex C_XN_Y species at higher temperatures. These complexes decompose near 700 K to produce N_2 and CO. There are no desorption products that contain both C and N.

Introduction

Reduced cerium oxide (CeO_X) has been shown to dramatically alter the activity of molecules adsorbed on supported Rh. NO and CO dissociate more readily on Rh/CeO_X than on single-crystal Rh.[1−6] When NO and CO are coadsorbed, the molecules and their component atoms interact on the Rh surface resulting in new surface species that are not observed on the pure metal.[7]

The enhanced NO dissociation activity is potentially beneficial for the catalytic reduction of NO in exhaust streams. However, as the NO decomposes the CeO_X is oxidized which ultimately poisons the enhanced dissociation. A reductant must be added to maintain the reduced CeO_X. H_2 and CO are likely candidates; however, under UHV conditions they do not remove oxygen from CeO_X to produce either H_2O or CO_2.[1,3]

Hydrocarbons are also promising candidates as reductants. Ferrizz et al.[8] have shown that C_2H_4 adsorbed on Rh/CeO_X/yttria-stabilized zirconia (YSZ(100)) produced CO and CO_2. This demonstrates that C_2H_4 is a good reductant on Rh/CeO_X whereas H_2 and CO are not.

The next step is to study how NO and C_2H_4 interact on Rh/CeO_X. The reaction between NO and C_2H_4 has been extensively studied on Rh(111) in a series of papers by van Hardeveld et al.[9−12] H_2, H_2O, NO, CO, N_2, and HCN were observed in temperature-programmed desorption (TPD). The branching of the various reaction pathways that lead to these products was shown to be highly dependent on the relative coverage of NO and C_2H_4. High NO/C_2H_4 ratios favored the formation of H_2O, N_2, and CO_2. When the proportion of C_2H_4 was increased, the amount of H_2 and HCN increased while the amount of N_2 and CO_2 declined.

The presence of CeO_X alters the reaction pathways observed on the Rh. As previously seen, NO dissociation increases on Rh/CeO_X compared to NO on Rh(111). CeO_X may also participate directly in the reactions. Reduced CeO_X can remove oxygen from the Rh particles[3] while oxidized CeO_2 can supply oxygen.[8]

In this study, the reaction products that result from the coadsorption of NO and C_2H_4 on Rh/CeO_X are studied by TPD. C 1s and N 1s soft X-ray photoelectron spectroscopy (SXPS) was used to identify the surface intermediates that occur along the reaction path. Highly ordered ceria films were grown with the desired oxidation state in situ.[13] The cerium oxidation state was determined by core-level photoemission. The reactions on Rh/CeO_X are similar to those observed on Rh(111); however, there are important differences in both the products observed and the kinetics of the reactions. These differences are discussed in relation to the effect/participation of the CeO_X.

The interaction between atomic C and N on reduced Rh/CeO_X was previously studied by first dissociating CO and then adsorbing NO.[7] This system is compared to what is observed when NO interacts with C_2H_4. CO does not dissociate on oxidized Rh/CeO_2. The present system provides the first opportunity to study the interaction between C and N on Rh in the presence of oxidized ceria.

Experimental Section

The experiments were performed in two different UHV chambers.[14] The temperature-programmed desorption (TPD) experiments were performed in a chamber at ORNL. The temperature was ramped at 3 K/s and the sample was biased −70 V to prevent electrons generated by the mass spectrometer ionizer from stimulating reactions at the surface. Soft X-ray photoelectron spectroscopy (SXPS) was performed in a chamber at the National Synchrotron Light Source. Experiments were conducted on beamline U12A. C 1s and N 1s spectra were recorded using 405 and 525 eV excitation, respectively. The instrumental resolution was ca. 0.5 eV.

$CeO_X(111)$ films were grown in situ on Ru(0001) as previously described.[13] The ceria films were estimated to be ca. 5 nm thick based on the attenuation of the Ru 3d XPS intensity. The oxidation state of the Ce was controlled by first depositing a fully oxidized $CeO_2(111)$ film while the Ru was at 700 K. The oxygen pressure was then reduced and additional ceria was deposited. After deposition the sample was annealed to 900 K.

* Corresponding Author. David R. Mullins, Oak Ridge National Laboratory, P.O. Box 2008, MS 6201, Oak Ridge, TN 37831-6201. Phone: 865-574-2796. Fax: 865-576-5235. E-mail: mullinsdr@ornl.gov.

10.1021/jp0038411 CCC: $20.00
Published on Web 01/25/2001

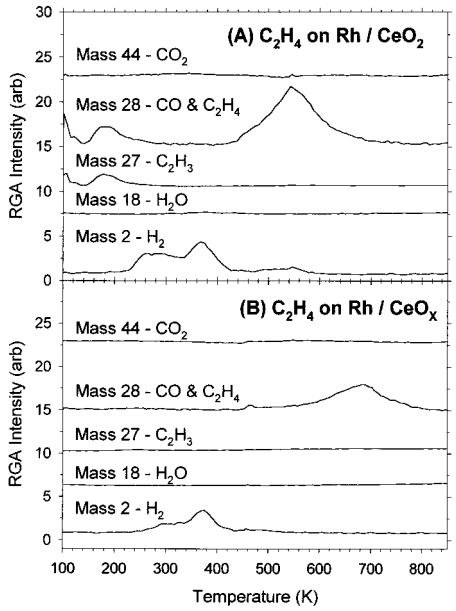

Figure 1. Temperature-programmed desorption spectra from a large exposure of C_2H_4 on Rh on (A) oxidized, and (B) reduced CeO_X.

The average oxidation state was determined by the Ce 3d, Ce 4d, or valance band photoemission spectra.[15] Two limiting cases were examined. Samples referred to as oxidized had fully reduced Rh deposited on oxidized ceria containing more than 95% Ce^{4+} ($CeO_{1.98}$). Samples referred to as reduced had fully reduced Rh deposited on reduced ceria containing less than 25% Ce^{4+} ($CeO_{1.63}$).

Rh was deposited from a resistively heated evaporative source while the sample was maintained at 300 K. After deposition the sample was heated to 900 K. The Rh flux was monitored by a mass spectrometer. The same Rh exposure was used for all TPD experiments and for all SXPS experiments. The relative amount of Rh between the TPD and XPS experiments is believed to be similar. The Rh coverage was estimated to be 5×10^{14} cm^{-2} (±50%) based on the Rh 3d SXPS intensity compared to the Ru 3d SXPS intensity for clean Ru and the attenuation of the Ce 4d SXPS intensity following Rh deposition. The Rh agglomerates slightly upon annealing from 300 to 900 K as indicated by a decrease in the Rh AES and XPS intensities. The Rh surface area was determined by comparing the CO TPD intensity from the deposited Rh compared to CO from clean Ru(0001). The Rh surface area was ca. 0.25 ML relative to the Ru(0001).

$^{15}N^{16}O$ (Cambridge Isotope Labs) or $^{14}N^{16}O$ (Matheson) and C_2H_4 (Matheson) were adsorbed from separate directional dosers.[16] The use of $^{15}N^{16}O$ allowed $^{15}N_2$ to be differentiated from CO while $^{14}N^{16}O$ allowed $^{14}NH_3$ to be differentiated from H_2O and $HC^{14}N$ to be differentiated from CO. Unless otherwise indicated the gases were dosed to ensure saturation, i.e., further exposure resulted in no changes in the SXPS or TPD spectra. The typical exposure was approximately equal to 20 L.

Results

C_2H_4 or NO on Rh/CeO_X. The adsorption of C_2H_4[8] or NO[1,2] adsorbed separately on Rh/CeO_X have been discussed before. The data are presented here for comparison to the coadsorption case. Temperature-programmed desorption spectra from C_2H_4 adsorbed on Rh supported by highly oxidized or by highly reduced CeO_X are shown in Figure 1, parts A and B, respectively. If no Rh is present, the C_2H_4 desorbs below 150 K and exhibits no decomposition (data not shown). The C_2H_4 was adsorbed at 150 K on both the oxidized and reduced samples, but the reduced sample was annealed to 200 K before the TPD (Figure 1B). The only desorption products observed are CO, H_2, and C_2H_4. In particular, no H_2O or CO_2 was observed. The C_2H_4, as seen in the cracking fragment at 27 amu, desorbs below 200 K. The pre-anneal before the TPD eliminated the C_2H_4 desorption in Figure 1B.

H_2 exhibits a broad desorption from 240 to 420 K with a peak at 370 K. There is also a small H_2 desorption near 550 K (Figure 1A). The H_2 desorption is consistent with what has been observed for C_2H_4 on Rh(111). The desorption from 250 to 350 K reflects the loss of hydrogen as C_2H_4 converts to ethylidyne, CCH_3.[17] The H_2 desorption from 350 to 420 K results from the decomposition of the ethylidyne. The small amount of desorption between 500 and 600 K may result from either the decomposition of more stable hydrocarbon fragments[17] or from the decomposition of hydroxyl groups on the CeO_X.[14] Similar features were observed by Ferrizz et al. on Rh/CeO_X/YSZ(100).[8] There are no significant shifts in the H_2 desorption spectra between the oxidized and reduced samples.

CO desorbs in a peak centered at 540 K on the oxidized sample (Figure 1A) and at 690 K on the reduced sample (Figure 1B). The CO desorption results from the oxidation of C on the Rh by O in the ceria. CO desorption is therefore not seen on Rh(111). The CO peak positions are consistent with those observed by Ferriz et al. on Rh/CeO_X/YSZ(100).[8]

The H_2 and CO desorption intensity decreased by ca. 50% on the reduced sample compared to the oxidized sample. Ferriz et al. attributed a similar decrease to a morphology change in the Rh upon heating to 900 K.[8] In the present case, both samples were heated to 900 K before C_2H_4 was adsorbed. The decrease therefore suggests a difference in the Rh induced by the oxidation state of the substrate.

C 1s core-level SXPS spectra from C_2H_4 on Rh on oxidized and reduced CeO_X are shown in Figure 2, parts A and B, respectively. The spectra recorded after annealing to temperatures from 150 to 400 K are similar for the two samples. A single, symmetric peak at 284.2 eV dominates the spectra at 150 K. This peak is assigned to C_2H_4. The C 1s signal becomes broader and asymmetric at 200 K. Two peaks near 284.2 and 285 eV are clearly evident at 300 K. The peaks have been assigned to the non-hydrogenated and hydrogenated C atoms in ethylidyne, respectively.[18] The appearance of intensity below 284 eV accompanies the further dehydrogenation that starts near 350 K. The peak below 284 eV may be associated with the hydrogenated C in acetylide, CCH.[19] After the H_2 desorption is complete near 400 K, the C 1s spectra contain a single peak, assigned to atomic C, at 284.3 eV.[3] The atomic C disappears between 500 and 600 K on the oxidized sample and between 700 and 800 K on the reduced sample. There is no evidence of CO, which has a binding energy near 287 eV.[3]

The TPD following NO adsorption on Rh on oxidized and reduced CeO_X are shown in Figure 3. N_2 and NO both desorb from the oxidized sample (Figure 3a). The onset of N_2 desorption coincides with the peak of the NO desorption at 400 K. This suggests that NO decomposition competes with NO desorption. Some of the NO desorption between 200 and 350 K comes from NO adsorbed on the CeO_2.[20] Virtually no NO desorbs from the reduced sample (Figure 3B) and what is observed desorbs from the CeO_X not the Rh.[2,20] The N_2 desorption from 240 to 450 K results primarily from the decomposition of NO on CeO_X.[2,20] The N_2 from the decomposi-

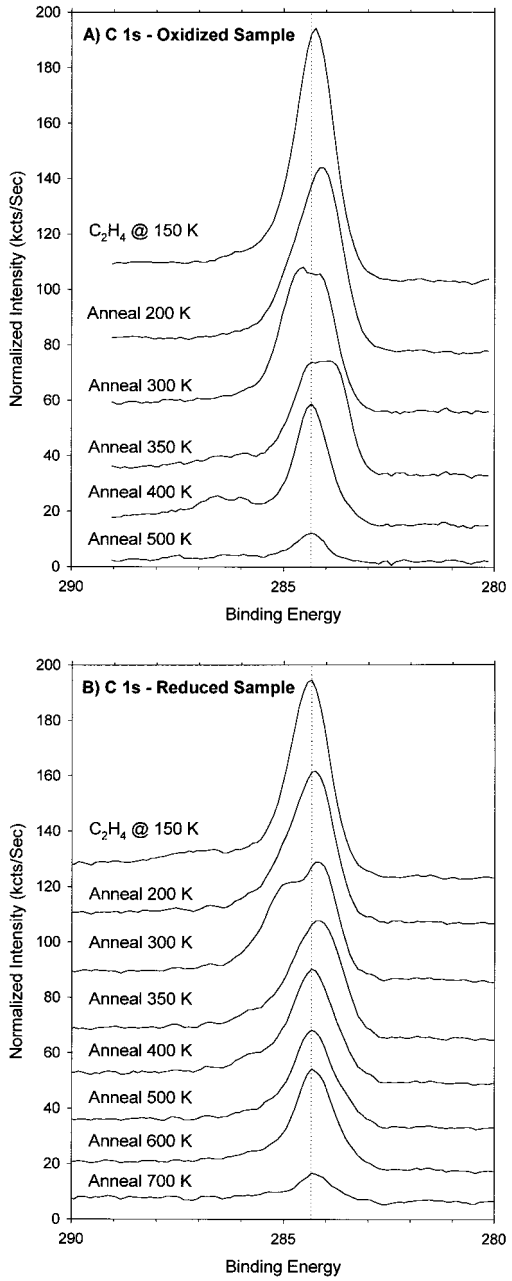

Figure 2. C 1s photoemission spectra from a large exposure of C_2H_4 on Rh on (A) oxidized, and (B) reduced CeO_X. C_2H_4 was exposed at 150 K and then annealed as indicated.

tion of NO on the Rh particles occurs in a broad desorption from 450 to 800 K with a maximum desorption rate at 560 K. The high-temperature N_2 desorption contains a small contribution resulting from the decomposition of nitride near 500 K.[20]

The thermal evolution of the N 1s SXPS spectra is shown in Figure 4. Two N 1s peaks are seen on the oxidized sample (Figure 4A). The higher binding energy peak at 401 eV is assigned to NO on Rh while the peak at 398 eV results from N on Rh.[2] The NO desorbs and decomposes between 300 and 400 K. The atomic N increases significantly as the NO decomposes. The atomic N disappears between 600 and 700 K.

The N 1s spectra from the reduced sample (Figure 4B) are more complex due to the interaction of NO with CeO_X.[20] The peaks from NO and N on Rh appear at the same binding energy as in Figure 4A, but new peaks at 402.2 and 396.2 eV result from NO^- and N^{3-} on CeO_X, respectively. As the sample is heated, the atomic N on Rh grows as the NO dissociates. The

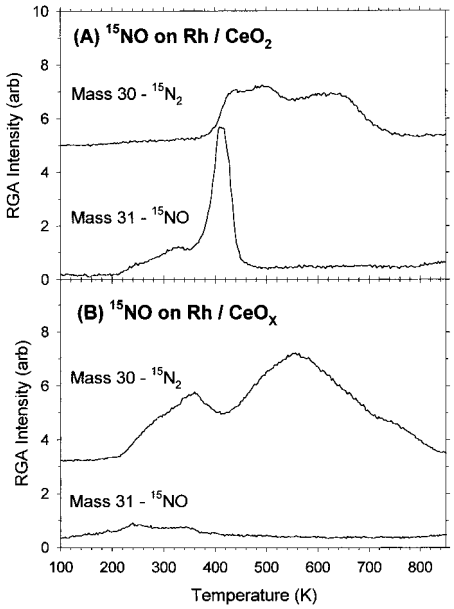

Figure 3. Temperature-programmed desorption spectra from a large exposure of ^{15}NO on Rh on (A) oxidized, and (B) reduced CeO_X.

decomposition of NO to form atomic N occurs at a lower temperature and to a greater extent on the reduced sample compared to the oxidized sample.[2] All of the NO is gone by 400 K and the N disappears between 600 and 700 K.

Coadsorption on Rh/Oxidized CeO_2. The interaction between C_2H_4 and NO on Rh(111) is highly dependent on the relative coverages of the two adsorbates.[9] Due to design differences in the gas dosers in the two vacuum chambers, it was difficult to reproduce the gas exposures in the two systems. The most reproducible means of coadsorbing the two molecules was to expose the sample to an excess of C_2H_4, ca. 20 L, followed by a similar exposure to NO. This allowed the C_2H_4 and NO to coadsorb on the Rh/CeO_X. If the adsorbates were exposed in the reverse order, i.e., the surface was first saturated with NO, then no C_2H_4 was adsorbed on the sample.

The TPD following C_2H_4 adsorption at 150 K and NO adsorption at 200 K on Rh on oxidized CeO_2 is shown in Figure 5. ^{15}NO was used in the experiment shown in Figure 5A and ^{14}NO was used in Figure 5B. The principal desorption products are N_2, NO, CO, and H_2O. Comparing Mass 28 in Figure 5A and Mass 27 in Figure 5B, it is clear that the small peak near 250 K is due to C_2H_4 and not CO. Mass 27 could also be due to H^{14}N. However, HCN would only be expected to desorb above 300 K following NO and C_2H_4 decomposition. As shown in Figure 5B, no HCN is evident in the Mass 27 desorption. The weak Mass 17 feature near 420 K (Figure 5B) is a cracking fragment from H_2O and is not indicative of NH_3 formation. A broad, weak CO_2 peak may be present near 600 K. There is no H_2 desorption.

The CO desorption is very similar to what was produced by C_2H_4 without NO (Figure 1A), although the peak is shifted to slightly higher temperature, 580 K compared to 550 K. Less NO is desorbed relative to N_2 compared to what resulted from NO adsorption without C_2H_4 (Figure 3A). The NO desorption still occurs at 400 K but the majority of the N_2 desorption occurs above 600 K.

The C 1s spectrum for C_2H_4 coadsorbed with NO on an oxidized sample at low temperature (Figure 6A) is similar to that for C_2H_4 without NO (Figure 2A). However, at 300 K, ethylidyne is evident in the absence of NO but is not when NO is coadsorbed. At 400 K the C has largely dehydrogenated in

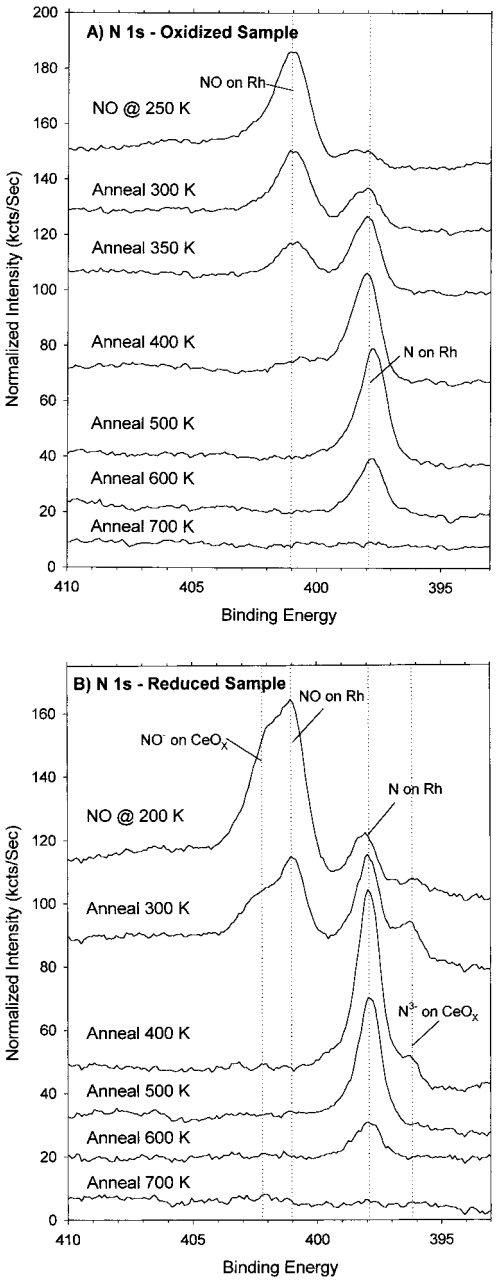

Figure 4. N 1s photoemission spectra from a large exposure of NO on Rh on (A) oxidized, and (B) reduced CeO_X. NO was exposed at (A) 250 K or (B) 200 K and then annealed as indicated.

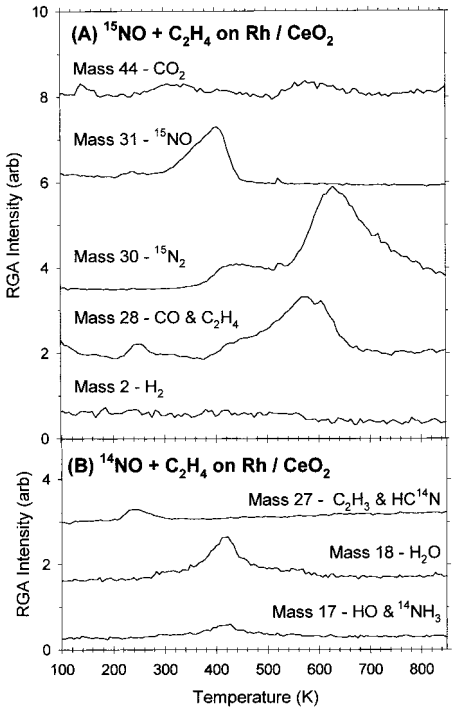

Figure 5. Temperature-programmed desorption spectra from a large exposure of C_2H_4 at 150 K followed by (A) ^{15}NO or (B) ^{14}NO at 200 K on Rh on oxidized CeO_2.

both systems as indicated by the single peak that is shifted to slightly higher binding energy compared to the spectra at lower temperatures. The decrease in the C 1s intensity is indicative of CO desorption, but no CO or CO_2 is observed on the surface. No C remains on the surface above 600 K.

No new features appear in N 1s spectra when NO is coadsorbed with C_2H_4 on Rh/CeO_2 (Figure 6B) compared to NO adsorbed by itself (Figure 4A). However, there is no decomposition of NO evident at 300 K in Figure 6B and there is still NO on the surface at 400 K. This indicates an inhibition of NO decomposition by the C_2H_4.

Coadsorption on Rh/Reduced CeO_X. The TPD from C_2H_4 and NO coadsorbed on Rh on reduced CeO_X is shown in Figure 7. ^{15}NO was used in Figure 7A and ^{14}NO was used in Figure 7B. The primary desorption products are N_2, CO, and H_2. A small amount of C_2H_4 desorbs at low temperature as on the oxidized sample and a broad CO_2 desorption possibly occurs near 600 K. There is no NO, H_2O, HCN, or C_2N_2 produced. The small amount of Mass 17 near 410 K is assigned to NH_3 since Mass 18 indicates that there is no water desorption.

The H_2 desorption is similar to what was observed in the absence of NO (Figure 1B). A broad desorption occurs from 250 to 350 K followed by a sharper peak at 400 K. A higher temperature desorption state is more clearly evident at 520 K. The CO desorption is divided into two states: a lower-temperature plateau from 500 to 650 K, followed by a more intense peak at 720 K. The N_2 desorption is divided into two well-separated states. The low-temperature state that has a peak near 370 K is from the decomposition of NO on CeO_X. The high-temperature state at 720 K comes from N on the Rh particles.

The C 1s and N 1s spectra for C_2H_4 and NO coadsorbed on the reduced sample are shown in Figure 8, parts A and B, respectively. There is little interaction evident between the coadsorbates below 400 K. The C 1s spectra are consistent with the stepwise dehydrogenation of ethylene as seen in Figure 2B. The features associated with ethylidyne at 300 K are not as evident in Figure 8A but the peak is significantly broader than what is seen at 200 K and presumably is composed of emission from various C species. At 400 K the N 1s spectrum indicates the presence of only N on Rh and N^{3-} on CeO_X.

New peaks appear in both spectra at 500 K and above that are associated with bonding between C and N. These peaks were also observed when NO and CO were coadsorbed on reduced Rh/CeO_X.[7] The C 1s peak at 287 eV and the N 1s peak that re-appears at 400.8 eV are assigned to CN. The CN features fade as the sample is heated to 700 K. Two peaks emerge in the C 1s spectra that are assigned to a more complex C−N species. The difference in binding energy between C_XN_Y(I) and C_XN_Y(II) is related to differences in the C−N bond hybridization and/or the number of N atoms bonded to the C.[7,21] Multiple peaks are not as evident in the N 1s spectrum at 700 K but the N 1s signal is shifted and asymmetric compared to the N/Rh

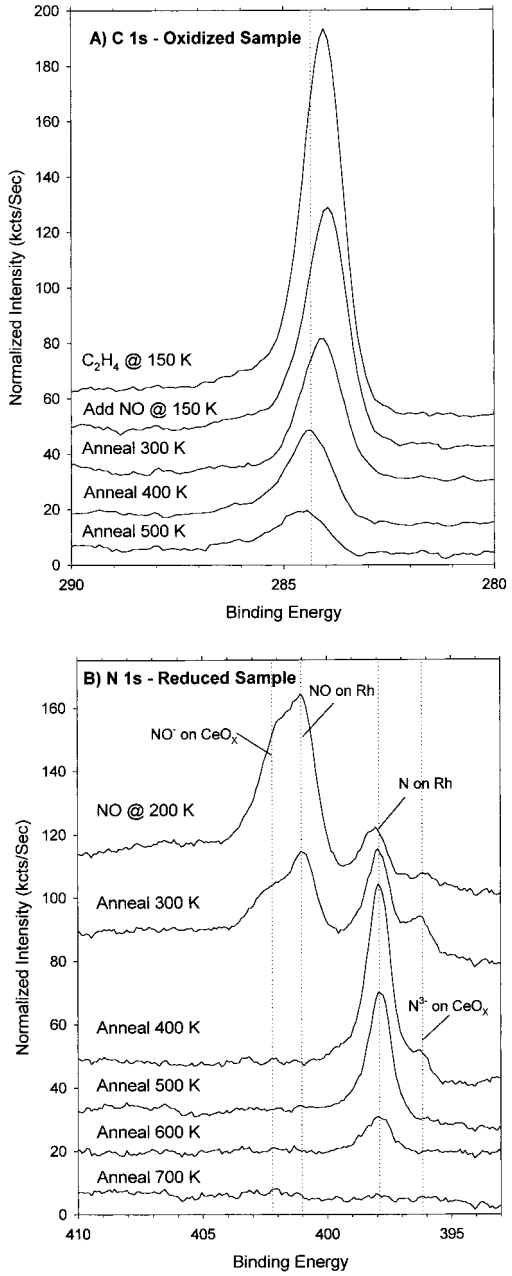

Figure 6. (A) C 1s and (B) N 1s spectra from a large exposure of C_2H_4 at 150 K followed by NO at 150 K on Rh on oxidized CeO_2 and then annealed as indicated.

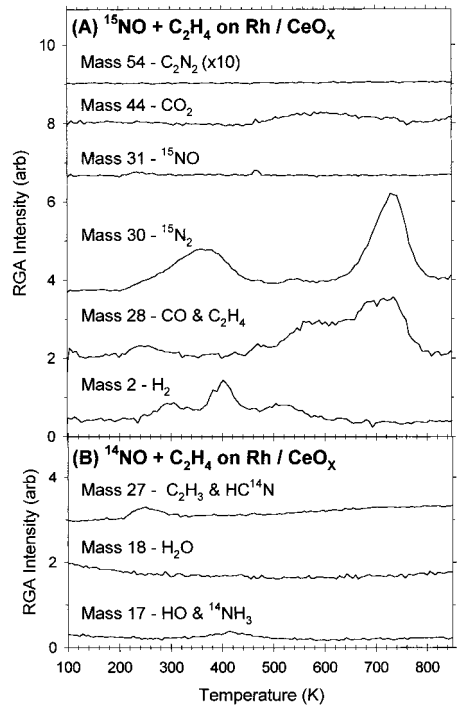

Figure 7. Temperature-programmed desorption spectra from a large exposure of C_2H_4 at 150 K followed by (A) ^{15}NO or (B) ^{14}NO at 200 K on Rh on reduced CeO_X.

peak that is observed at lower temperatures. All of the C 1s and N 1s signal disappears after annealing to 800 K.

Discussion

The reaction of C_2H_4 and NO on Rh(111) can produce a number of products including H_2, H_2O, HCN, CO, N_2, NO, and CO_2.[9] A general reaction pathway is shown in Scheme 1. Branching along the pathway and the relative amounts of the various products are dependent on the relative amounts of C_2H_4 and NO.[9] A larger relative amount of NO leads to the formation of more N_2 and CO_2. A larger relative amount of C_2H_4 leads to more HCN and H_2O.

The presence of the reducible oxide CeO_X alters the reaction path in a number of ways. The primary effects can be understood by considering the CeO_X as an additional reactant. It can provide oxygen, resulting in CO from C adsorbed on Rh, and also remove oxygen, thus eliminating pathways that might lead to H_2O or CO_2. Reduced ceria also promotes the decomposition of NO on Rh[1,2] thus reducing the amount of NO desorbed.

The reaction between C_2H_4 and NO on oxidized Rh/CeO_2 is summarized in Scheme 2. The absence of H_2 and HCN in Figure 5 indicates that the O from the decomposition of NO consumes all of the H from the decomposition of C_2H_4. Note that in Figure 1 the H from C_2H_4 does not react with the O in the CeO_2. There are no surface intermediates formed between C and N on Rh/CeO_2 even though CN intermediates were detected on Rh(111)[9] and Rh/CeO_X.[7] The existence of C and N atoms on the Rh particles is therefore not sufficient to ensure CN intermediates. This may be a coverage effect since it has been shown on Rh(111) that an excess of NO leads to N_2 at the expense of CN. However, in the present system a large amount of C_2H_4 was adsorbed on the Rh before the NO so it is unlikely that the CN formation is limited by the availability of C. Alternatively, the lack of a C−N interaction may be due to the competition of C reacting with O in the CeO_2. Temperatures sufficient to promote the reaction between C and N are also sufficient to initiate the C−O reaction and the oxidation reaction is apparently more favorable.

In the present experiments it is not possible to differentiate CO formed from O from CeO_2 vs O from NO. Isotopically labeled oxygen in the NO might provide this information. However, the CO desorption has a prominent peak at 580 K and a low-temperature tail from 400 to 500 K. From a comparison with the coadsorption of C_2H_4 + NO on Rh(111),[9] the low temperature portion can be tentatively assigned to the reaction of C with O from NO. Similarly, from a comparison with C_2H_4 on Rh/CeO_2 (Figure 1A) the high-temperature peak can be assigned to the reaction of C with the oxide. The small amount of CO_2 formed indicates that there is not an excess of O on the surface from NO. As seen in Figure 1 and in the desorption of CO from Rh/CeO_2,[4,5] CO can form readily from the reaction of C with CeO_2 but further oxidation to CO_2 is not favored.

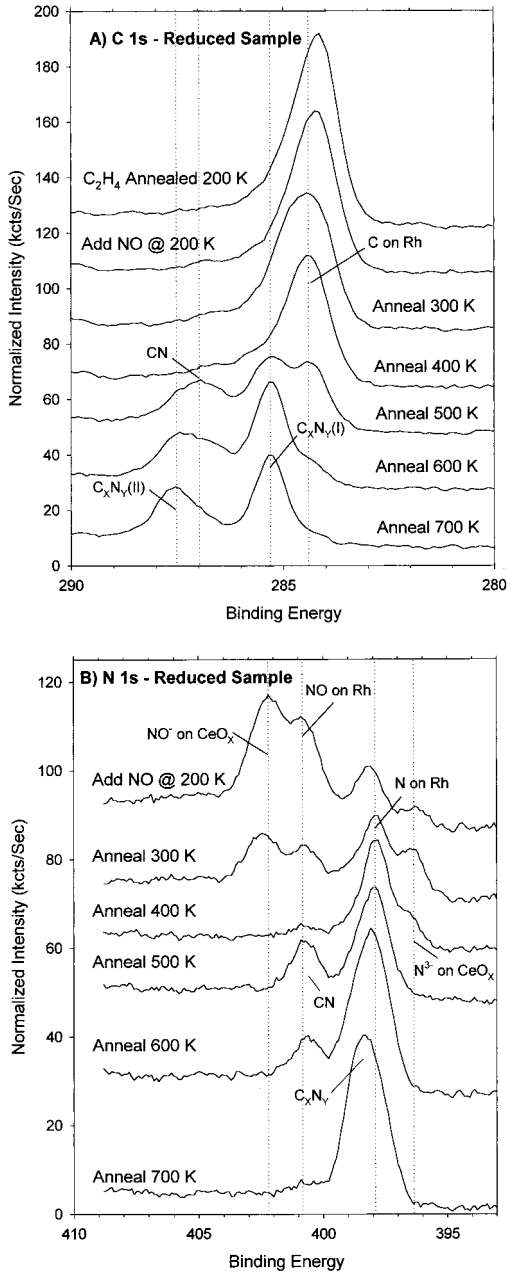

Figure 8. (A) C 1s and (B) N 1s spectra from a large exposure of C_2H_4 at 200 K followed by NO at 200 K on Rh on reduced CeO_X and then annealed as indicated.

It is not clear why the N_2 desorption is shifted to higher temperatures. Van Hardeveld et al. suggested that the shift of N_2 desorption to higher temperatures when NO was coadsorbed with C_2H_4 on Rh(111) resulted from the formation and decomposition of CN on the surface. The SXPS spectra in Figure 6 demonstrate that this is not the case in the current system. Even though the C and N do not react with each other, perhaps the C atoms occupy adsorption sites that block the reaction of N with other N atoms. This hypothesis is consistent with the results in Figure 5 where the N_2 desorption comes after the C is removed from the surface in CO(g).

When C_2H_4 and NO are coadsorbed on reduced Rh/CeO_X the reduced ceria acts to remove O from the Rh particles. As shown in Figure 8b, the NO has significantly dissociated by 300 K. However, the reappearance of H_2 and the absence of H_2O in Figure 7 indicate that the O is removed from the Rh below 400 K. The reduced sample also promotes the dissociation of NO hence the absence of desorbed NO in Figure 7a. The

SCHEME 1: C_2H_4 + NO on Rh(111)

$C_2H_4(a) + NO(a)$

$H_2(g)$ ↙ ; ↓ 100 K - 300 K

$C_XH_Y(a) + NO(a)$

$H_2(g), H_2O(g)$ ↙ ; ↓ 300 K - 400 K

$C_XH_Y(a) + NO(a) + N(a)$

$CO(g), CO_2(g), H_2(g), H_2O(g), NO(g)$ ↙ ; ↓ 400 K - 500 K

$C_XH_Y(a) + C(a) + N(a)$

$HCN(g), N_2(g)$ ↙ ; ↓ 500 K - 600 K

$CN(a) + C(a)$

↓ 600 K - 900 K

$N_2(g) + C_2N_2(g) + C(a)$

reaction pathway on the reduced sample is summarized in Scheme 3. A small amount of NH_3 is observed but no HCN. HCN but no NH_3 was produced on Rh(111) following the reaction C_2H_4 with N.[12] Apparently the C is stabilized on Rh/CeO_X and therefore the formation of HCN is not favorable.

Above 400 K the C 1s and N 1s spectra (Figure 8) are very similar to what was observed during the reaction of NO and CO on Rh/CeO_X.[3] This is not surprising since above 400 K, NO and CO are dissociated and the O has diffused to the ceria. The surfaces are therefore essentially the same, consisting of C and N on the Rh particles. The absence of OCN at any temperature in the present system is a further indication that isocyanate forms from the reaction of CO and N on Rh/CeO_X.[3]

SCHEME 2: C_2H_4 + NO on Rh/CeO_2

$C_2H_4(a) + NO(a) + CeO_2$

$C_2H_4(g)$ ↙ ; ↓ 100 K - 300 K

$C_XH_Y(a) + H(a) + N(a) + O(a) + NO(a) + CeO_2$

$NO(g), H_2O(g)$ ↙ ; ↓ 300 K - 400 K

$C(a) + NO(a) + N(a) + O(a) + CeO_2$

$CO(g), N_2(g), NO(g)$ ↙ ; ↓ 400 K - 500 K

$C(a) + N(a) + CeO_2$

↓ 500 K - 700 K

$N_2(g) + CO(g) + CeO_{2-\delta}$

SCHEME 3: C_2H_4 + NO on Rh/CeO_X

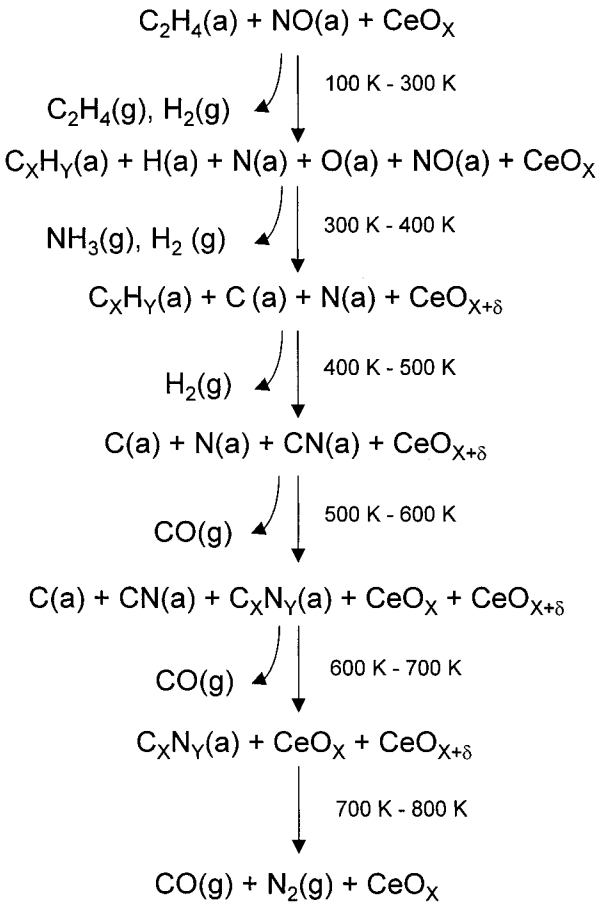

As observed before, C and N first form CN and then at higher temperatures form more complex C−N species. The CO desorption between 500 and 600 K results from the reaction of atomic C with CeO_X. The CO and N_2 desorption above 700 K follows the decomposition of the C_XN_Y species. No C_2N_2 desorption was observed, presumably because the reaction of C with CeO_X is more favorable than the desorption of C_2N_2.

Conclusion

C_2H_4 can serve as a partner in the catalytic reduction of NO over Rh/CeO_X. In a detailed understanding of the mechanism, CeO_X serves as the reductant for the decomposition of NO. C_2H_4 then acts to reduce the CeO_2 back to CeO_X. In principle, the ratio of NO to C_2H_4 could be balanced so that ceria would remain reduced and highly active. C_XN_Y intermediates are formed on the Rh/CeO_X. These species are more stable than C or N on Rh/CeO_2 and therefore a higher temperature is required to keep the Rh/CeO_X clean and active.

Acknowledgment. Research sponsored by the Division of Chemical Sciences, Geosciences, and Biosciences, Office of Basic Energy Sciences, U.S. Department of Energy, under contract DE-AC05-00OR22725 with Oak Ridge National Laboratory, managed and operated by UT-Battelle, LLC, and in part by an appointment to the Oak Ridge National Laboratory Postdoctoral Research Associates Program administered jointly by the Oak Ridge Institute for Science and Education and Oak Ridge National Laboratory. The National Synchrotron Light Source, Brookhaven National Laboratory, is supported by the U.S. Department of Energy, Division of Materials Sciences and Division of Chemical Sciences.

References and Notes

(1) Overbury, S. H.; Huntley, D. R.; Mullins, D. R.; Ailey, K. S.; Radulovic, P. V. *J. Vac. Sci. Technol.* **1997**, *A15*, 1647.
(2) Overbury, S. H.; Mullins, D. R.; Kundakovic, Lj. *Surf. Sci.*, submitted.
(3) Mullins, D. R.; Overbury, S. H. *J. Catal.* **1999**, *188*, 340.
(4) Stubenrauch, J.; Vohs, J. M.; *J. Catal.* **1996**, *159*, 50.
(5) Putna, E. S.; Gorte, R. J.; Vohs, J. M.; Grahm, G. W. *J. Catal.* **1998**, *178*, 598.
(6) Stubenrauch, J.; Vohs, J. M. *Catal. Lett.* **1997**, *47*, 21.
(7) Mullins, D. R.; Kundakovic, Lj.; Overbury, S. H. *J. Catal.* **2000**, *195*, 169.
(8) Ferrizz, R. M.; Egami T.; Vohs, J. M. *Catal. Lett.* **1999**, *61*, 33.
(9) van Hardeveld, R. M.; Schmidt, A. J. G. W.; Niemantsverdriet, J. W. *Catal. Lett.* **1996**, *41*, 125.
(10) Niemantsverdriet, J. W.; Borg, H. J.; van Hardeveld, R. M.; van Santen, R. A. *Recl. Trav. Chim. Pays-Bas* **1996**, *115*, 486.
(11) van Hardeveld, R. M.; Schmidt, A. J. G. W.; van Santen, R. A.; Niemantsverdriet, J. W. *J. Vac. Sci. Technol.* **1997**, *A 15*, 1642.
(12) van Hardeveld, R. M.; van Santen; R. A.; Niemantsverdriet, J. W. *J. Phys. Chem. B* **1997**, *101*, 7901.
(13) Mullins, D. R.; Radulovic, P. V.; Overbury, S. H. *Surf. Sci.* **1999**, *429*, 186.
(14) Kundakovic, Lj.; Mullins, D. R.; Overbury, S. H. *Surf. Sci.* **2000**, *457*, 51.
(15) Mullins, D. R.; Overbury, S. H.; Huntley, D. R. *Surf. Sci.* **1998**, *409*, 307.
(16) Overbury, S. H.; Mullins, D. R.; Huntley, D. R.; Kundakovic, Lj. *J. Phys. Chem. B* **1999**, *103*, 11308.
(17) Borg, H. J.; van Hardeveld, R. M.; Niemantsverdriet, J. W. *J. Chem. Soc., Faraday Trans.* **1995**, *91*, 3679.
(18) Andersen, J. N.; Beutler, A.; Sorensen, S. L.; Nyholm, R.; Setlik, B.; Heskett, D. *Chem. Phys. Lett.* **1997**, *269*, 371.
(19) Heskett, D. Private communication.
(20) Overbury, S. H.; Mullins, D. R.; Huntley, D. R.; Kundakovic, Lj. *J. Catal.* **1999**, *186*, 296.
(21) Ronning, C.; Feldermann, H.; Merk, R.; Hofsäss, H.; Reinke, P.; Thiele, J.-U. *Phys. Rev. B* **1998**, *58*, 2207.